



Interseismic Coupling, Megathrust Earthquakes and Seismic Swarms Along the Chilean Subduction Zone (38°–18°S)

M. MÉTOIS,¹ C. VIGNY,² and A. SOCQUET³

Abstract—The recent expansion of dense GPS networks over plate boundaries allows for remarkably precise mapping of interseismic coupling along active faults. The interseismic coupling coefficient is related to the ratio between slipping velocity on the fault during the interseismic period and the long-term plates velocity, but the interpretation of coupling in terms of mechanical behavior of the fault is still unclear. Here, we investigate the link between coupling and seismicity over the Chilean subduction zone that ruptured three times in the last 5 years with major earthquakes (Maule Mw 8.8 in 2010, Iquique Mw 8.1 in 2014 and Illapel Mw 8.4 in 2015). We combine recent GPS data acquired over the margin (38°–18°S) with older data to get the first nearly continuous picture of the interseismic coupling variations on the subduction interface. Here, we show that at least six low coupling zones (LCZ), areas where coupling is low relatively to the neighboring highly coupled segments can be identified. We also find that for the three most recent Mw > 8 events, coseismic asperities correlate well with highly coupled segments, while LCZs behaved as barriers and stopped the ruptures. The relation between coupling and background seismicity in the interseismic period before the events is less clear. However, we note that swarm sequences are prone to occur in intermediate coupling areas at the transition between LCZ and neighboring segments, and that the background seismicity tends to concentrate on the downdip part of the seismogenic locked zone. Thus, highly coupled segments usually exhibit low background seismicity. In this overall context, the Metropolitan segment that partly ruptured during the 2015 Illapel earthquake appears as an outlier since both coupling and background seismicity were high before the rupture, raising the issue of the remaining seismic hazard in this very densely populated area.

Key words: Interseismic coupling, subduction zone, Chile, megathrust earthquakes, seismic swarms, segmentation.

Electronic supplementary material The online version of this article (doi:10.1007/s00024-016-1280-5) contains supplementary material, which is available to authorized users.

¹ Univ Lyon, Université Lyon 1, Ens de Lyon, CNRS, UMR 5276 LGL-TPE, 69622 Villeurbanne, France. E-mail: marianne.metois@univ-lyon1.fr

² Laboratoire de Géologie, UMR 8538, CNRS, Ecole Normale Supérieure Paris, PSL-Research University, 24 rue Lhomond, 75231 Paris cedex 05, France.

³ Institut des Sciences de la Terre, CNRS, Université Joseph Fourier, Université Grenoble-Alpes, Saint-Martin-d'Hères, France.

1. Introduction

GPS instrumentation along active plate boundaries has contributed significantly to better constrain the characteristics and mechanics of large destructive megathrust earthquakes. For instance, the coseismic slip of the Mw 8.8 2010 Maule earthquake that ruptured the South-Central part of the Chilean subduction zone has been precisely imaged using GPS data from local campaign networks installed since the early 1990s in the epicentral region (e.g., RUEGG *et al.* 2009; MORENO *et al.* 2010; MÉTOIS *et al.* 2012). The deformation of the sea floor off the Sendai coast measured by offshore geodesy brought unique insights on the shallow slip during the Tohoku Mw 9 2011 earthquake (e.g., SIMONS *et al.* 2011; SATO *et al.* 2011). Moreover, analysis of the seismicity or cGPS time-series before the 2011 Tohoku and the 2014 Mw 8.2 Iquique earthquakes show that anomalous activity was going on in the vicinity of these megathrust earthquakes, days or weeks before the rupture itself (e.g., KATO *et al.* 2012; RUIZ *et al.* 2014; SCHURR *et al.* 2014). Seismic and tsunami records have shown that the 2015 Mw 8.4 Illapel earthquake ruptured a shallow portion of the subduction zone (YE *et al.* 2015; ÁRANGUIZ *et al.* 2016; CALISTO *et al.* 2016), while GPS measurements conducted after the 2010 Maule earthquake show that the 2015 rupture area was affected by eastward postseismic motion, suggesting an indirect triggering between the Maule and Illapel earthquakes (RUIZ *et al.* 2016; KLEIN *et al.* 2016). Overall, the present-day challenge for the scientific community remains in the deep understanding of the mechanical behavior of the fault interface that should help identify zones of high seismic hazard between highly coupled segments

with low background seismicity, and more complex zones where precursory activity could develop before the occurrence of the next megathrust earthquake.

Over the last decades, geodetic measurements conducted during the interseismic phase along several subduction zones have provided maps of the upper-plate deformation that reflect the degree of locking between plates on the interface (e.g., CHLIEH *et al.* 2008; WALLACE *et al.* 2004; LOVELESS and MEADE 2011; MCCAFFREY 2002, 2014; YOSHIOKA *et al.* 2005; MORENO *et al.* 2008). However, these works often suffer from heterogeneous or sparse measurements and from the large distance between the coast and the trench (more than 200 km in Japan or Sumatra) that impede detailed mapping of the along-strike or along-dip variations of the coupling coefficient. Furthermore, although there seems to be a good correlation between interseismic coupling and seismic rupture in general (e.g., CHLIEH *et al.* 2008; KONCA *et al.* 2008; MORENO *et al.* 2010; MÉTOIS *et al.* 2012; LOVELESS and MEADE 2011; RUIZ *et al.* 2016), how kinematic coupling relates to the mechanical properties of the interface and to the shape and magnitude of the coming earthquakes are open questions that are still being actively discussed (e.g., MORENO *et al.* 2010; KANEKO *et al.* 2010; HETLAND and SIMONS 2010).

The fast Nazca–South America convergence zone [~ 68 mm/year (e.g., VIGNY *et al.* 2009; ARGUS *et al.* 2011)], where little partitioning occurs but that is seismically very active (one $M_w > 8$ every 10 years in average, but already three since 2010) is a suitable place to determine interseismic coupling and to investigate its relation with mechanical properties of the interface and characteristics of the upper and downgoing plates. In particular, because the distance between the coast and the trench is smaller than elsewhere (around 100 km and up to 70 km locally), the Chilean subduction zone is a good candidate for such study, because it allows a good resolution almost up to the trench. Hence, we build for the first time a nearly continuous map of interseismic coupling along this subduction zone (38° – 18° S) that we compare with the slip distributions of the 2010 (Maule), 2014 (Iquique) and 2015 (Illapel) $M_w > 8$ megathrust earthquakes and with the “background” seismicity, i.e., the moderate-magnitude earthquakes that occurred on the plate interface before the main shocks.

2. Tectonic Context

In the following, we consider the Chilean margin deformation at a very large scale, along a ~ 3000 -km-long portion of the subduction between the Nazca and South American plates, from 38° to 18° S. Therefore, the margin’s distinctive features (e.g., slab geometry, trench sedimentation style, nature and structure of the upper and downgoing plates, volcanic activity) significantly vary from South to North in our study area (see HOFFMANN-ROTHER *et al.* 2006 for a review). In particular, the Andean mountain belt resulting from the long-term deformation of South America is more than 450 km wide from 18° S to 26° S where it is characterized by the ~ 3500 -m-high Altiplano-Puna plateau to the North and the Subandean active fold-and-thrust belt on its eastern front (Fig. 1, ARMIJO *et al.* 2010). The main belt is less complex and is only 150 km wide south of 33° S, with no clear eastern front and no uplifted plateau. From 26° to 33° S in Central Chile, the principal cordillera is relatively sharp while the wide Sierras Pampeanas diffuse deformation area develops to the East with several active thrust fronts (e.g., REILINGER and KADINSKY-CADE 1985; BROOKS *et al.* 2003).

The coastal cordillera is separated from the principal cordillera by the central valley in the North (18° – 24° S) and South-Central Chile (32° – 38° S). In South-Central Chile, the western front of the Andes has been described as an active crustal thrust (ARMIJO *et al.* 2010; VARGAS *et al.* 2014). Central Chile (24° – 32° S) appears again as an outlier in this overall pattern since the transition from the coastal to principal cordillera is smooth, i.e., the central valley vanishes. This peculiar region overlays the deep Pampean flat-slab area where the Nazca plate flattens at ~ 100 km depth and where no subduction-associated volcanism is observed (TASSARA *et al.* 2006; MAROT *et al.* 2014). Closer to the trench, we observe smaller scale (several tens of kilometers) variations of the Chilean coast morphology like large bays (e.g., La Serena or Baranquilla bays) and peninsulas (e.g., Arauco or Mejillones peninsula), the latter being often associated with complex crustal fault networks (e.g., MELNICK and BOOKHAGEN 2009; ARMIJO and THIELE 1990).

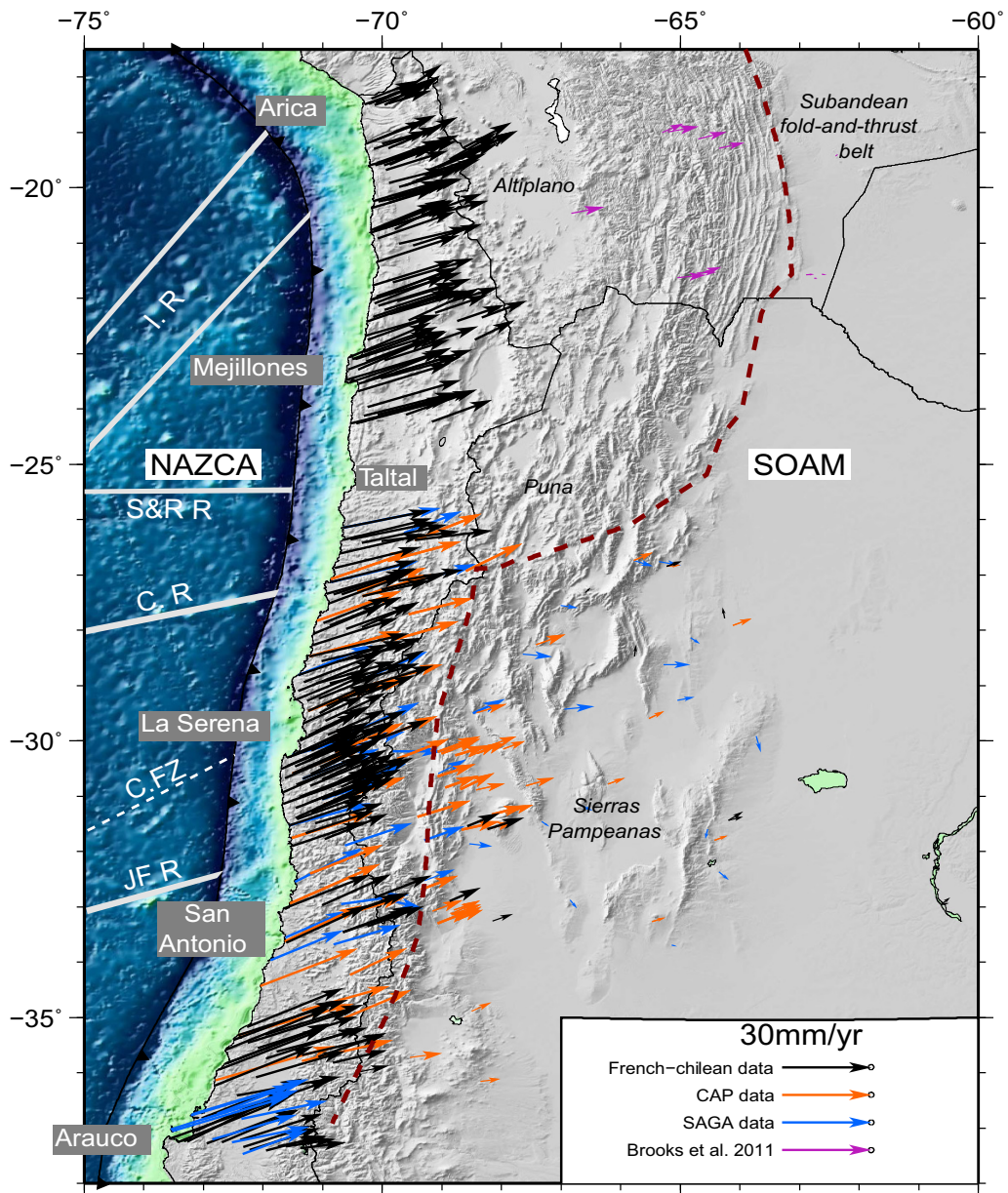


Figure 1

Combined horizontal velocity field from continuous and campaign GPS measurements plotted relative to stable South America (defined by NNR-Nuvel1A DeMETS *et al.* 1994). CAP is the name of the US experiment (BROOKS *et al.* 2003; BEVIS *et al.* 1999); SAGA is the GFZ experiment (KLOTZ *et al.* 2001; KHAZARADZE and KLOTZ 2003). Dashed brown line rough border of the eastern edge of the Andean sliver. White lines major bathymetric features of the Nazca plate (HOFs). I.R. Iquique Ridge, S&R R. Sala y Gomez Ridge (or Taltal ridge), C.R. Copiapo ridge, C.F.Z. challenger fracture zone, J.F.R. Juan Fernandez ridge

The Nazca plate characteristics also vary from North to South Chile: first, the subducted oceanic crust is younger in the South than in the North [45 Ma at 18°S and 28 Ma at 38°S (MULLER *et al.* 1997)]

implying large differences in the thermal state of the lithosphere; second, the plate is deformed by volcanic ridges and fractures (high oceanic features or HOFs) with different orientations and wave lengths (Fig. 1).

Besides all these lateral variations, the deformation of the entire region is dominated by the seismic cycle on the subduction interface that accommodates one of the highest convergent rates on Earth (68 mm/year). As can be seen in Fig. 2 where the moderate-size seismicity registered by the CSN (Centro Sismológico Nacional, <http://www.sismologia.cl/>) during the interseismic phase is plotted, the seismic activity illuminates the subduction interface down to 600 km depth, while only few earthquakes are recorded on shallow crustal structures. The exact

amount of the Nazca–South America convergence that could be taken by these secondary active faults is still an open question, but it seems reasonable to assume that an overall 80–90 % of the Chilean margin deformation is associated with the subduction fault from 38°S to 18°S. The 1 cm/year velocity gradient observed across the subandean fold-and-thrust belt and its seismic activity led several authors to propose an Andean sliver independent from the South American craton that would absorb the remaining 10–20 % relative motion (see Fig. 1,

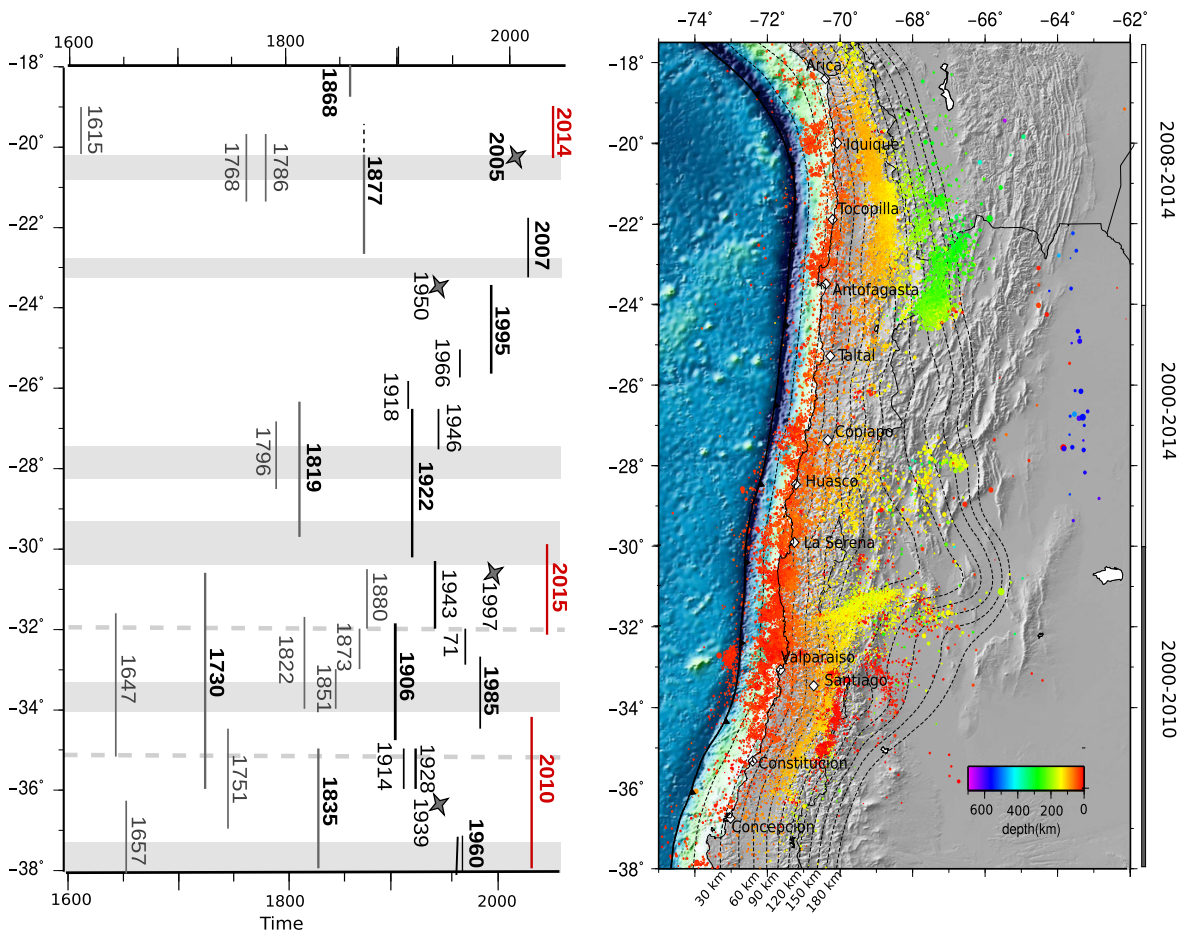


Figure 2

Left estimated extent of large historical or instrumental ruptures along the Chilean margin adapted from Métois et al. (2012). Gray stars mark major intra-slab events. The recent $M_w > 8$ earthquakes are indicated in red. Gray shaded areas correspond to LCZs defined in Fig. 3. Right seismicity recorded by the Centro Sismológico Nacional (CSN) during interseismic period, color-coded depending on the event's depth. Three zones have been defined to avoid including aftershocks and preshocks associated with major events: (1) in North Chile, we plot the seismicity from 2008 to January 2014, i.e., between the Tocopilla and Iquique earthquakes; (2) in Central Chile, we plot the seismicity from the entire 2000–2014 period; (3) in South-Central Chile, we selected events that occurred between 2000 and 2010, i.e., before the Maule earthquake

KENDRICK *et al.* 2001; BROOKS *et al.* 2003, 2011; CHLIEH *et al.* 2011; MÉTOIS *et al.* 2013, 2014; NOCQUET *et al.* 2014).

3. Interseismic Velocity Field

GPS measurements have been conducted by international teams in Chile since the early 1990s both on survey and permanent networks (s- and c-GPS, respectively), providing us with interseismic velocities measured over 20 years in some places (BEVIS *et al.* 2001, 2003; BROOKS *et al.* 2011; KHAZARADZE and KLOTZ 2003; KLOTZ *et al.* 2001; RUEGG *et al.* 2009; VIGNY *et al.* 2009; BÉJAR-PIZARRO *et al.* 2009; CHLIEH *et al.* 2011). After the destructive 2010 Maule earthquake, a large instrumentation effort has been conducted over North and Central Chile (18°–35°S) that provides us with unusually dense present-day measurements of interseismic loading on the interface over a 3- to 5-year time-span. Now, because of the two additional mega-thrust earthquakes in 2014 (Mw 8.1, Iquique) and 2015 (Mw 8.4, Illapel), that produced large co-seismic displacements and ongoing post-seismic deformation, it will not be possible to further refine the inter-seismic coupling in these areas. Therefore, the data collected before these large earthquakes are the only way to understand the pre-existing strain and stress state of the Chilean interface to date.

We combine the data published by RUEGG *et al.* (2009) and MÉTOIS *et al.* (2013, 2014) to produce a consistent velocity field that homogeneously covers the 3000-km-long portion of the plate boundary (18°–38°S), with the exception of a small gap in the Atacama desert area that still lacks measurements (24.3°–25.5°S). The resulting data set is formed of 248 recent horizontal GPS velocities that we combined together with most of the previously published data sets in South-Central Chile (see MÉTOIS *et al.* 2012 for further details). We thus gather 396 horizontal velocities into a single data set (Fig. 1) that we complete with 70 reliable vertical velocities (see supplementary figure 1).

This velocity field is heterogeneous since each data-set has been calculated on a different time-span: for instance, the interseismic velocities published by

RUEGG *et al.* (2009) in the Maule area result from the 1996–2002 period, while the velocities published by MÉTOIS *et al.* (2013) in North Chile are derived from measurements made from 2008 to 2013. In order to remove from our data set the velocities potentially affected by the 1960 earthquake postseismic motion still presently ongoing, we chose to exclude the velocities published by KLOTZ *et al.* (2001) south of 34°S and the velocities published by MORENO *et al.* (2008) south of 38°S in the 1960 epicentral area. Therefore, despite the fact that they are determined over different time windows, we are confident that all velocities presented in Fig. 1 are “interseismic”, i.e., are representative of the average deformation over several years before the occurrence of large ruptures on the megathrust interface.

The overall deformation pattern shown on Fig. 1 relative to the stable South America as defined by NNR-Nuvel1A (DEMETTS *et al.* 1994) is typical of the deformation expected from interseismic loading on a buried dislocation, at least at the first order (OKADA 1985). Indeed, velocities are roughly parallel to the plate convergence in the near field, while they decrease and rotate towards a more trench perpendicular direction going inland and reach a null velocity in the South American craton. Additional non-negligible north-eastward deformation (~ 1 cm/year) is observed in the backarc, in particular in the Sierras Pampeanas and in the Altiplano Andes where only few mm per year should be observed in a purely elastic frame.

4. Modelling of GPS Data

We use the Tdefnode code developed by MCCAFFREY (2009) based on backslip assumption and Okada’s equations (OKADA 1985; SAVAGE 1983) to invert for the coupling distribution that best reproduces these data. We choose to simultaneously invert for the rigid rotation of an Andean sliver that would afford for part of the backarc deformation since it decreases significantly the normalized root mean square (nRMS) of the inversion and has been proposed by several previous works (BROOKS *et al.* 2003; MÉTOIS *et al.* 2013; NOCQUET *et al.* 2014). We present simpler 2-plate models for comparison in

supplementary figures 5 and 7. Therefore, we assume that nearly all the observed deformation is elastic and due to the seismic cycle on the subduction interface, neglecting the small-scale deformation that could be produced by loading on second-order crustal faults (see Sect. 2) but that is not detected by our regional campaign networks. For instance, the San Ramon active fault located at the edge of the Santiago basin is supposed to be loaded at 0.4 mm/year (ARMJO *et al.* 2010), a rate that is well beyond the s-GPS resolution. Similarly, the available data spanning the Sierras Pampeanas are too sparse to enable the detection of accumulation of elastic deformation on individual thrust faults. Therefore, we include this complex area in the South American plate and consider the westernmost thrust front as the eastern boundary of the Andean sliver (Fig. 1).

We divided the slab interface into a grid of 93 along-strike nodes (every 0.25°) and 11 along-dip nodes (every 7.5 km depth) based on the realistic Slab 1.0 geometry (HAYES *et al.* 2012). We use 862 independent observations to invert simultaneously for coupling on each nodes and the three parameters of the sliver Euler pole. To avoid numerical instabilities, we impose a 2D (both along strike and dip) smoothing regularization that allows for the best compromise between small-scale coupling variations and fit to the data [shape spread smoothing technique proposed by McCaffrey (2009)]. To limit the number of free parameters, we force the rake of the backslip component to be parallel to the plate convergence velocity.

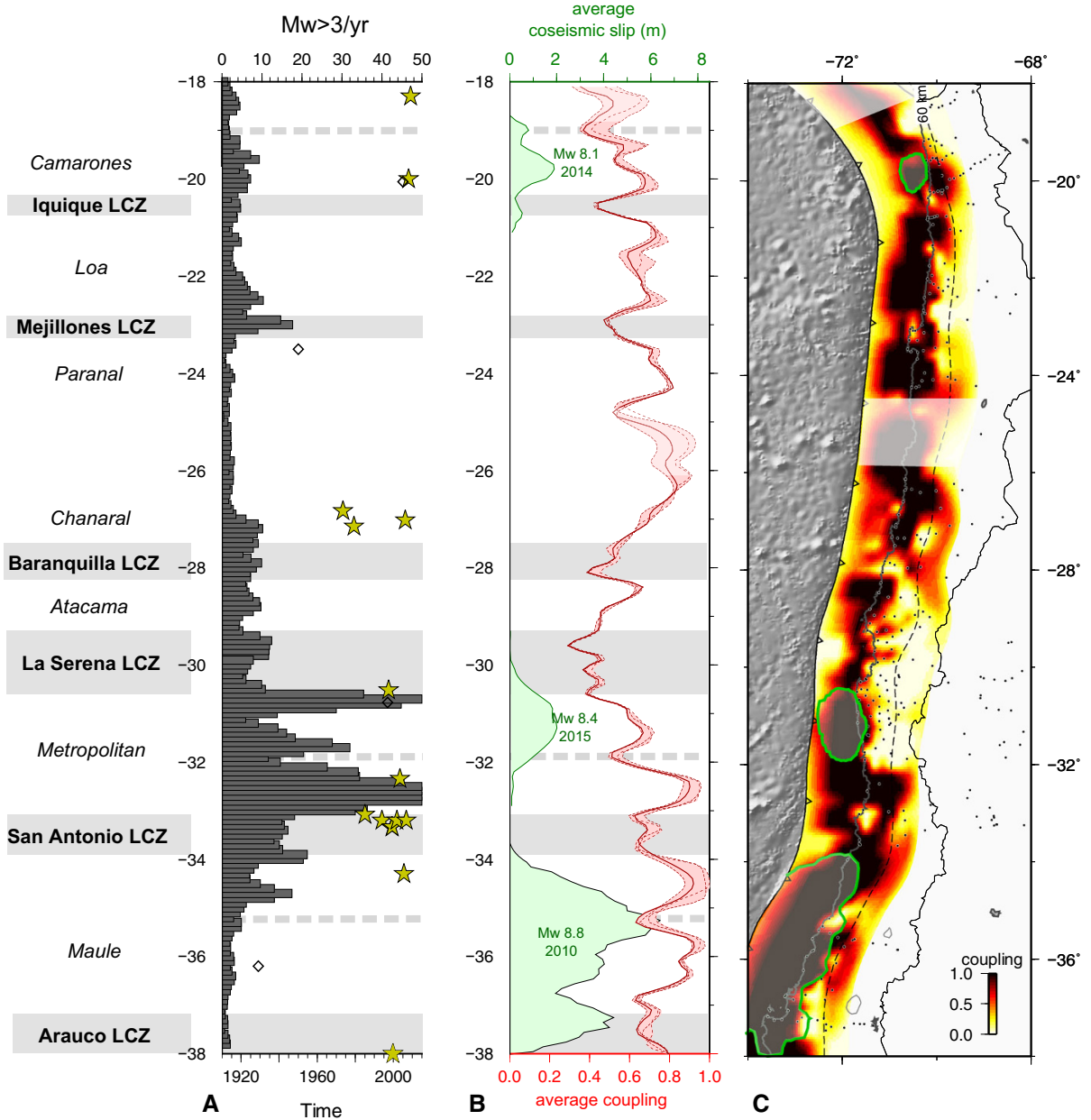
We estimate the sensitivity of our data set to unit displacements on each node of the grid by summing the horizontal deformation on the whole network following Loveless and Meade (2011) (see supplementary figure 2 and checkerboard tests in supplementary figure 3). The “power” of our horizontal data to constrain the coupling on the interface is high from 15 km depth to more than 70 km depth in general. In areas where the measurements are very dense, i.e., from 33°S to 26°S , resolution is good nearly up to the trench. We lack resolution mainly on the edges of our model (in the Arica bend, and south of Arauco peninsula) and in the very shallow part of the subduction interface. Lack of measurements in the Taltal area (from 25°S to 26°S) makes the

Figure 3

a Histogram depicts the rate of $M_w > 3$ earthquakes registered by the CSN catalog during the interseismic period defined for each zone (see Fig. 2) on the subduction interface, on 0.2° of latitude sliding windows. Stars are swarm-like sequences detected by Holtkamp *et al.* (2011) depending on their occurrence date. Swarms located in the Iquique LCZ and Camarones segment are from Ruiz *et al.* (2014). Empty squares are significant intraplate earthquakes. **b** Red curve variations of the average coupling coefficient on the first 60 km of depth calculated on 0.2° of latitude sliding windows for our best model including an Andean sliver motion. Dashed pink curves are alternative models with different smoothing options that fit the data with nRMS better than 2 (see supplementary figure 6); the pink shaded envelope around our best model stands for the variability of the coupling along strike. Green curves coseismic distribution for Maule (Vigny *et al.* 2011), Iquique (Lay *et al.* 2014) and Illapel earthquakes (Ruiz *et al.* 2016). Gray shaded areas stand for the identified low coupling zones (LCZs). LCZs and high coupling segments are named on the left. The apparent decrease in the average coupling North of 30°S is considered as an artifact of the Andean sliver motion (see Sect. 5.2). **c** Best coupling distribution obtained inverting for Andean sliver motion and coupling amount simultaneously. The rupture zones for the three major earthquakes are indicated as green ellipses. White shaded areas are zones where we lack resolution

coupling unresolved in this region (see Fig. 3c). Recent instrumentation efforts should bring soon new clues about interseismic loading there. Based on this sensitivity test, it is important to note that coupling models are not—or barely—resolved in the first tens of kilometers of the slab. In other words, constraining the coupling value on these shallow nodes to either 0 or 100 % does not impact the nRMS of the inversion. Therefore, using coupling models for generating tsunami scenarios that are mainly influenced by the shallow slip distribution is still challenging, even if promising results have been found for the Illapel earthquake where the coupling resolution is high even in the shallowest part of the slab (e.g., Calisto *et al.* 2016).

Our best coupling distribution (see Fig. 3c) reproduces well the data set with an nRMS around 1.6 for the horizontal velocities, and 2 for the vertical velocities. We find that the data require a rotation motion of the Andean sliver around an Eulerian pole given by 56.37°S , 41.27°W and $-0.12^\circ/\text{Myr}$ relative to stable South America (as defined by NNR-NuvellA DeMets *et al.* 1994) in close agreement with the pole determined in more local studies (Métois *et al.* 2013, 2014). This results in a ~ 8 mm/year translation-like motion of the Altiplano towards the



North East in Northern Chile that decreases to less than 5 mm/year in the backarc area of the Maule region where the subandean active front is no longer visible. If the Andean range is a rigid microplate, this would imply that a significant part of the Nazca–

South America convergence is taken on the active subandean fold-and-thrust belt, reducing the total amount of potentially accumulated displacement on the subduction interface (NORABUENA *et al.* 1998; CHLIEH *et al.* 2011; BROOKS *et al.* 2011).

5. Discussion

5.1. Kinematics of the Nazca–South America Convergence

We model the surface deformation as a combination of elastic deformation coming from loading on the subduction interface and the rigid rotation of the so-called “Andean sliver” block. This modeling trick retrieves well the velocities observed in the Bolivian subandean fold and thrust belt (BROOKS *et al.* 2011) and produces more realistic coupling distribution than a simpler 2-plate model since no or little coupling is needed deeper than 60 km depth to retrieve the velocities observed (see supplementary figures 5 and 7).

However, such a rigid block model and elastic approach has some limitations. First, the eastern boundary of the Andean sliver is not well defined south of 26°S since no clear dominant active front has been detected in the Sierras Pampeanas and South of them. The deformation in the Sierras Pampeanas is diffuse and taken by several active structures and therefore cannot be retrieved using an elastic block model approach. As a result, our best model fails to retrieve the details of the deformation in this region (supplementary figure 4). Second, it is well known now that a large part of the interseismic deformation observed in the middle to far field of rapid subduction zones can be explained by visco-elastic loading models as it has been proposed for North Chile (LI *et al.* 2015), Sumatra and Japan (TRUBIENKO *et al.* 2013). However, it is to note that the deformations predicted in the near field by both elastic and visco-elastic approach are similar (TRUBIENKO *et al.* 2013). Therefore, we are confident that our simple elastic model retrieves well the first-order pattern of deformation in the near field of the subduction fault and in particular the small-scale along-strike variations of the coupling coefficient, but the sliver motion, the residual velocities observed in mid and far field (see supplementary figure 4), and the coupling distribution with depth have to be interpreted with extreme caution.

Despite these limitations and keeping them in mind, it is interesting to note that the Euler pole found for the Andean Sliver implies a decreasing

backarc shortening rate from North to South Chile and an overall clockwise rotation of the entire sliver. These broad characteristics of the deformation are in agreement with several paleomagnetic studies that have been conducted in the last decades (e.g., ARRIAGADA *et al.* 2008), and suggest that the deformation averaged in the region since Paleogene may still be going on today. Another argument in favor of a persistent motion of the Andean block on long time-scale is the fact that residuals pointing North are observed in the mid-field in Central Chile (supplementary figure 4) suggesting that the North-Eastward block motion imposed by our inversion does not account for part of the deformation in the North–South direction in this region. This northward motion in the Central Chile principal cordillera has been also described in the cumulated deformation pattern observed over several million years (ARRIAGADA *et al.* 2008).

5.2. The Chilean Margin is Segmented

The small-scale along-strike variations of the amount of coupling are preserved whatever the smoothing coefficient and shortening amount taken by the sliver motion, and therefore considered robust (Fig. 3b and supplementary figure 5). The along-dip variations of the coupling coefficient are less well constrained since they mainly impact the vertical deformation pattern that is poorly known compared to the horizontal deformation (see supplementary figure 1). InSAR images offering dense measurements of the upper plate deformation dominated by the vertical signal, together with continuous GPS data could help constraining better the downdip extent of the highly coupled zone (e.g., BÉJAR-PIZARRO *et al.* 2009; DUCRET *et al.* 2012). Overall, the highly coupled zones ($\Phi > 80\%$) do not extend below 60 km depth. Whether these nearly locked patches spread up to the trench is beyond the resolution of our model (see Sect. 4).

We define the average coupling at a given position along the trench as the integration of the coupling coefficient over depth, from surface to 60 km depth, i.e., the supposed downdip limit of the seismogenic zone. The profile of the average coupling versus latitude shown in Fig. 3b images a succession of seven

large highly coupled segments bounded by six narrow low coupled zones (LCZ). We define these LCZs as areas of abrupt decrease in the average coupling surrounded by zones where coupling is higher and relatively stable. Since a single threshold value valid for the entire trench could not be identified, the definition of an LCZ is local. Some LCZs are associated with a clear interruption of the highly locked zone in map view (Baranquilla, Iquique, see Fig. 3c) while the locked zone only narrows in others (La Serena, San Antonio, Mejillones). In addition to the six clearest LCZs, three other areas exhibit a slight decrease in average coupling: in front of Constitución ($\sim 35^\circ\text{S}$, already identified by MORENO *et al.* (2010)), another in front of Los Vilos ($\sim 32^\circ\text{S}$), and finally offshore Arica ($\sim 18^\circ\text{S}$). These features have not been always detected in previous works and appear more model-dependent than the others (in particular, they are barely visible in the 2-plate models, see supplementary figure 7). This is probably due to the fact that they are characterized by a decrease in the coupling on the 30–60 km depth part of the interface, i.e., they are associated with a sharpening of the transition zone from the deep creeping portion to the shallow zone that remains highly coupled. Conversely, in most of the other LCZs, coupling decreases even in the shallowest part of the fault. The Los Vilos LCZ ($\sim 32^\circ\text{S}$) also correlates with an abrupt change in the slab geometry that flattens at 100 km depth and an important increase in the background seismicity rate (Fig. 2).

The comparison between the average coupling calculated for 2-plate and 3-plate models (supplementary figure 5) shows that the segmentation of the margin (small-scale along-strike variations) is preserved while the average coupling tends to decrease significantly North of 24°S in the 3-plate models. This may be due to the fact that the Andean block motion in this area decreases the effective convergence rate on the subduction interface by 1 cm/year, or to the fact that the coupling values are lower in the shallowest unresolved part of the interface in the 3-plate models than in the 2-plate models. Thus, we interpret this large-scale decrease of the average coupling as an artifact coming from our modeling strategy rather than a true feature that would correlate with changes in the subduction style for instance.

The recent establishment of interseismic coupling maps along several subduction zones has enlightened that along-strike and along-dip variations of the coupling coefficient are common features that may come from general characteristics of these plate boundaries. For instance, WANG and BILEK (2014) claim that LCZs correlate with the subduction of major bathymetric features of the subducted plate, while BÉJAR-PIZARRO *et al.* (2013) relate coupling coefficient to geological and tectonic complexities of the upper plate. In Chile, 5 of the 6 well-identified LCZs correlate with the subduction of ridges or fracture zones of the Nazca plate (high oceanic features, or HOFs) that enters into subduction (Iquique, Baranquilla, La Serena, San Antonio and Arauco LCZs), and all of them are associated with singularities in the coast-line morphology (peninsulas, bays) often related to crustal fault networks. Whatever the hypothesis considered, the correlation between coupling calculated from interseismic velocities acquired on few years of measurement and long-term geological and morphological features is a strong argument in favor of a relative stability in time and space of the interseismic coupling segmentation. Mechanical models considering the interaction between both plates during several seismic cycles should help in the future to tackle this issue. In any case, in Chile, most of the HOFs that are thought to control the coupling coefficient are oblique relative to the convergence velocity between both plates and should therefore be migrating significantly along the trench even at the time scale of several seismic cycles, challenging the hypothesis of a long-term structural control of coupling by HOFs.

In the following, we do not concentrate on the factors controlling the variations of the coupling coefficient but rather focus on the interpretation of the coupling maps in terms of mechanical behavior of the interface.

5.3. Segmentation and Megathrusts

Rupture zones of historical megathrust earthquakes documented in Chile since the eighteenth century (e.g., LOMNITZ 1970; COMTE and PARDO 1991) often correlate with highly coupled segments, suggesting that the zones where apparent interseismic

coupling is high are regions of velocity-weakening behavior (Fig. 2). On the other hand, LCZs are seldom crossed by megathrust ruptures and often behave as barriers to their propagation (KANEKO *et al.* 2010): more than 60 % of the historical major ruptures in Chile are stopped or initiated near LCZs while no more than 15 % propagated through them.

Only giant earthquakes seem to make their way through some very low-coupling regions like the 1730 or 1922 Mw ~ 9 events. These zones where the average coupling can reach values as low as 40 % could therefore be associated with areas of velocity-strengthening behavior, i.e., able to slow down or stop rupture propagation. This correlation between coupling and mechanical behavior should be carefully considered because of the stress-shadow effect produced by locked velocity-weakening areas in their vicinity that may lead to apparent high coupling in velocity-strengthening zones (e.g., BÜRGMANN *et al.* 2005; HETLAND and SIMONS 2010; MÉTOIS *et al.* 2012). In other words: a small LCZ may be invisible in the upper plate deformation pattern, if bounded by sufficiently large locked asperities.

The recent Maule (2010, Mw 8.8), Iquique (2014, Mw 8.1) and Illapel (2015, Mw 8.4) events allow for a detailed comparison of interseismic coupling with coseismic slip distributions. We plot in Fig. 3b both the average coupling and the average coseismic slip for each of these events, and in Fig. 4 their associated coseismic distribution by VIGNY *et al.* (2011), LAY *et al.* (2014) and RUIZ *et al.* (2016). As already shown by several authors for the Maule and Iquique earthquakes (MORENO *et al.* 2010; MÉTOIS *et al.* 2012; RUIZ *et al.* 2014; SCHURR *et al.* 2014), the first-order correlation between highly coupled segment and megathrust rupture is confirmed. In particular, all of these mega-earthquakes ruptures stopped when entering into an LCZ. In Fig. 5, we plot the coseismic slip versus the prevailing interseismic coupling Φ for each subfaults located in the megathrust ruptures zones and we calculate the conditional probability $P_{> 1.5\text{m}/\Phi}$ of experiencing more than 1.5 m of coseismic slip depending on the value of prevailing interseismic coupling Φ defined as:

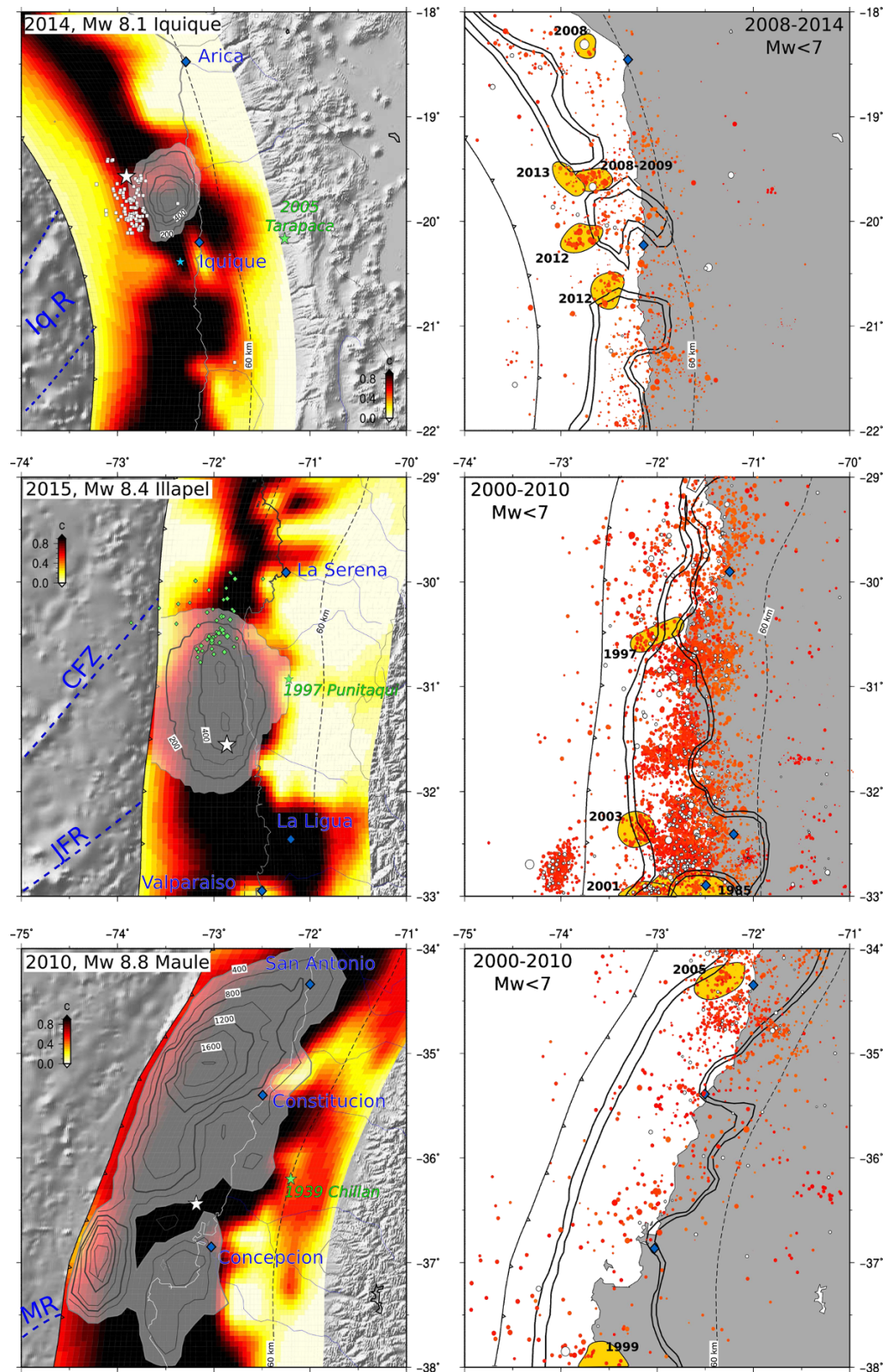
$$P_{> 1.5\text{m}/\Phi} = \frac{N_{\text{subfaults}_{> 1.5\text{m}/\Phi}}}{N_{\text{subfaults}_{\Phi}}}$$

Figure 4

Left coupling maps (color coded) versus coseismic slip distributions (gray shaded contours in cm) for the last three major Chilean earthquakes (epicenters are marked by white stars). From top to bottom Iquique area, white squares are pre-seismic swarm event in the month before the main shock, green star is the 2005, Tarapacá intraslab earthquake epicenter, blue star is the Mw 6.7 Iquique aftershock; Illapel area, green squares show the seismicity associated with the 1997 swarm following the Punitaqui intraslab earthquake (green star); Maule area, green star is the epicenter of the 1939 Chillan intraslab earthquake. Right interseismic background seismicity in the shallow part of the subduction zone (shallower than 60 km depth) for each region (red dots) together with 80 and 90 % coupling contours. White dots are events identified as mainshock after a declustering procedure following GARDNER and KNOPOFF (1974). Yellow areas extent of swarm sequences identified by HOLTKAMP *et al.* (2011) for South and Central Chile, and RUIZ *et al.* (2014) for North Chile

where N stands for the number of subfaults. These plots show that for all of three earthquakes, high coseismic slip is only observed in highly coupled subfaults, and that the correlation between the probability of experiencing more than 1.5 m of coseismic slip and the coupling Φ is ~ 90 % for the Maule and Illapel earthquakes. The Iquique case appears more complex since the coefficient of correlation is only 56 %. We interpret this lower correlation between prevailing interseismic coupling and the coseismic slip distribution for the Iquique earthquake as the result of the combined lack of resolution in the offshore part of the subduction interface for both coseismic and interseismic coupling models due to the large distance between the coast and the trench (~ 150 km). One other possible cause for the absence of striking correlation in the Iquique case is the fact that this event is relatively small compared to the Illapel and Maule events (Mw 8.1), and occurred in a swarm and slow slip context (e.g., RUIZ *et al.* 2014; SCHURR *et al.* 2014). It could be that the prevailing slow-slip event has released part of the slip that should have been released coseismically in a more standard megathrust rupture scenario, therefore biasing the correlation between interseismic coupling and coseismic slip.

Overall, in the case of the 2014 Iquique event, the earthquake ruptured the “Camarones” highly-coupled segment (in a region where the model resolution is lower than elsewhere) and has been stopped southward by the Iquique LCZ (RUIZ *et al.* 2014; SCHURR *et al.* 2014). The recent Illapel earthquake nucleated near a small LCZ at 32°S, ruptured the highly coupled patch



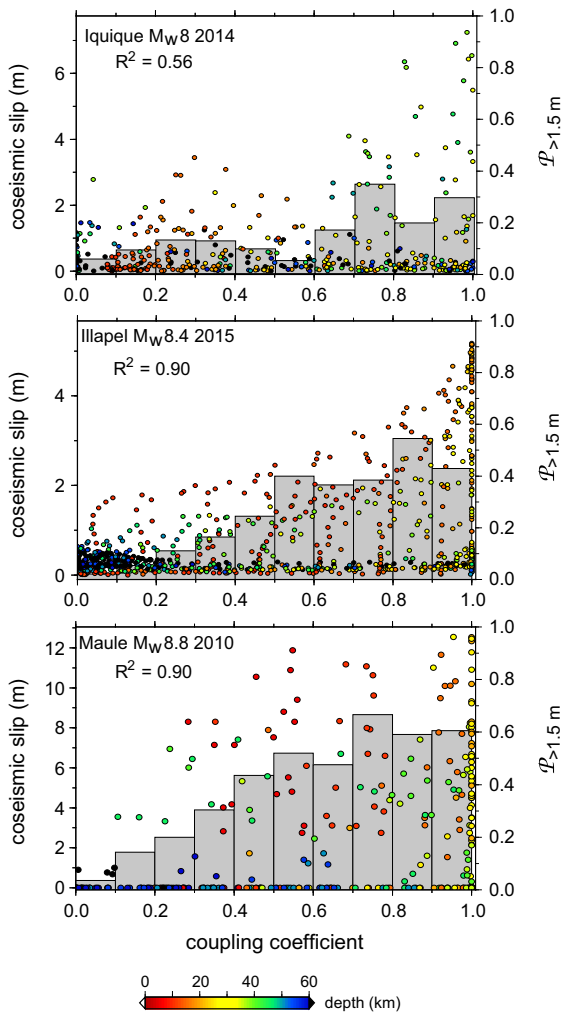


Figure 5

Correlation between coseismic slip amount and prevailing interseismic coupling for the three megathrust earthquakes that struck Chile since 2010. From *top to bottom*, case of: the Iquique Mw 8 2014, the Illapel Mw 8.4 2015 and the Maule Mw 8.8 2010 earthquakes. Coseismic slip and interseismic coupling for each subfault is represented by *dots, color-coded* depending on the subfault depth. The conditional probability of experiencing more than 1.5 m of coseismic slip depending on the prevailing coupling amount is represented by *gray histograms*. R^2 is the coefficient of correlation between $P_{(>1.5\text{m})/\phi}$ and the interseismic coupling calculated for each case

forming the northern part of the Metropolitan segment in between the subduction points of the Challenger fracture zone and of the Juan Fernandez ridge, and stopped northward at 30°S in the large La Serena LCZ (YE *et al.* 2015; RUIZ *et al.* 2016).

The Mw 8.8 Maule earthquake has a complex bi-lateral propagation that may reflect heterogeneities in

the pre-existing coupling or in the interface properties (MORENO *et al.* 2010; MÉTOIS *et al.* 2012) but also stopped at two LCZs: San Antonio in the North and Arauco in the South. An interesting feature of this earthquake is the very large coseismic slip observed in front of Constitución (35.2°S) where the average coupling calculated on the first 60 km depth is relatively low. This apparent contradiction has been interpreted by several authors as an evidence for dynamic propagation of the rupture through a previously creeping zone (MORENO *et al.* 2010), while other interseismic models were evidencing only a small decrease in the coupling coefficient at this latitude (MÉTOIS *et al.* 2012). However, as explained in Sect. 5.2, the highly coupled zone does not interrupt in the Constitución LCZ but is rather shallower and associated with a very sharp transition zone. To our opinion, this sharpening of the transition zone is consistent with an increase in coseismic slip in the upper portion of the interface. A possible scenario could be that the rupture coming from the South would have been unable to propagate in the 30–60 km deep portion of the interface since the transition zone was too sharp, thus increasing the stress on the highly coupled upper part of the fault, leading to a higher shallow coseismic slip.

Last but not least, the remaining unbroken portion of the Metropolitan segment is highly coupled (in fact was highly coupled before the Maule rupture) and should be considered with extreme caution: indeed there, stress has been increased by the neighboring ruptures but is simultaneously slowly released by viscous relaxation (KLEIN *et al.* 2016). However, this release rate is small compared to the long-term accumulation and the remaining high coupling zone could probably still rupture with an Mw > 8 event. Further detailed slip-budgets are difficult to conduct on the Chilean subduction zone because (1) the spatial resolution of all coseismic slip and interseismic slip models is limited, in particular in the shallowest part of the interface; (2) we lack insights on the slip distribution of the historical coseismic ruptures (namely the 1835, 1877 and 1922 earthquakes preceding the Maule, Iquique and Illapel earthquakes, respectively); and (3) we do not know today the portion of the plate convergence that could be accommodated by slow-slip events on the

subduction interface. In any case, based on the Chilean example, knowing the interseismic coupling allows for a rather good estimate of the size and shape of the coming ruptures, while the timing of such ruptures remains poorly understood.

5.4. *Interseismic Coupling and Background Seismicity*

All three $M_w > 8$ megathrust earthquakes that struck Chile in the last years were preceded by large intraplate events rupturing the oceanic slab between 60 and 120 km depth several years or decades before (Fig. 4). The Tarapacá M_w 7.8 earthquake ruptured in 2005 onshore of Iquique, the Chillán M_w 8.3 event devastated the Maule region in 1939 and the Punitaqui M_w 7.1 event was strongly felt in the Illapel area in 1997. The only other significant intraslab earthquake that has been reported over the margin is the deep 1950 Calama event that was followed by the shallower Antofagasta M_w 8 megathrust earthquake in 1995 (Fig. 2). This succession of large intraplate and large megathrust earthquakes raises the issue of a possible indirect triggering of megathrust ruptures (over tens of years) by changes in stress on the deep part of the subduction interface as suggested by KAUSEL and CAMPOS (1992) and BIE and RYDER (2015), or by a more complex triggering mechanism through a slow spread of deformation as observed in Greece (DURAND *et al.* 2014). More generally, it raises the question of the link between intraslab earthquakes, the background seismicity, the coupling and the megathrust rupture.

The first-order mechanical interpretation of interseismic coupling in the rate-and-state formalism implies that during interseismic loading, the LCZs should creep while the coupled segments should remain stuck. Therefore, aseismic transients should be registered near the LCZs. However, opposite to most of the world's subduction zones, no slow-slip event (SSE) has been observed along the Chilean subduction zone before the potential SSE that preceded the 2014 M_w 8.2 Iquique earthquake (RUIZ *et al.* 2014; SCHURR *et al.* 2014; LAY *et al.* 2014; KATO and NAKAGAWA 2014).

In order to better understand the mechanical behavior of the LCZs and segments, we analyzed the

background seismic activity ($3 < M_w < 7$ earthquakes) during the interseismic phase between two megathrust earthquakes based on the CSN catalog (<http://www.sismologia.cl/>, complete for $M_w > 3$ since 2000). We consider different periods representative of the interseismic background seismicity along the margin: from 2000 to 2010 for South-Central Chile (before the Maule event), from 2008 to 2014 for North Chile (between the Tarapaca and Iquique events), and from 2000 to 2014 for Central Chile (see Fig. 2). On Fig. 3a, where we plot the along-strike evolution of the seismicity rate together with the swarms that have been detected in Chile (HOLTKAMP *et al.* 2011; RUIZ *et al.* 2014), three seismic gaps, i.e., zones that experience very few moderate magnitude earthquakes, are clearly identified: the Maule, Loa and Paranal-Chanaral area that also correspond to highly coupled segments. No or few earthquakes occur where coupling is higher than 80 % (Fig. 4). In contrast, the Camarones segment was relatively active during the interseismic period even in the 80 % coupled zones, but seismicity and swarms (among which the preseismic sequence before the Iquique main shock see Fig. 4) mainly concentrate on the edges of the high coupling zone, near the Iquique LCZ. Finally, the Metropolitan segment is the most active portion of the Chilean subduction zone during the interseismic phase (Figs. 2, 4) with more than 50 $M_w > 3$ events per year on its edges, and at least 20 events per year in the highly coupled portion of the segment. The strong increase in seismicity rate between the Maule and Metropolitan segments appears correlated with the flattening of the deep portion of the slab.

Overall, it seems that higher seismicity rates are observed in or near the LCZs, while segments tend to be more silent during interseismic phase. However, the Metropolitan region behaves completely differently from this simple scheme since both seismicity and coupling are high. This first-order analysis conducted with the CSN catalog suffers obviously from the heterogeneity in the epicenters location accuracy, and from the completeness threshold of the catalog. More detailed and regional analysis are required to really conclude on the spatial relationship between moderate magnitude earthquakes and coupling.

However, interestingly, several swarm-like sequences occurring along the Chilean subduction zone have been recently pointed out by declustering methods applied to the CSN catalog (HOLTKAMP *et al.* 2011; RUIZ *et al.* 2014). Eight of these ten non-volcanic swarm sequences happen to be located at the transition zone between segments and LCZs (Figs. 2a, 4), in agreement with recent observations along other subduction zones (HOLTKAMP and BRUDZINSKI 2014). Little is known today about the kinematics and dynamics of these clusters that would require systematic relocation and analysis, but they emphasize a specific mechanical behavior of the subduction interface between segments and LCZs. It is to note that several of the shallowest swarms have been attributed to HOFs located in the shallow portion of the fault (e.g., COMTE *et al.* 2002; THIERER *et al.* 2005; CONTRERAS-REYES and CARRIZO 2011). For instance, the shallow seismic sequences located offshore San Antonio and Valparaíso (32°–34°S) are thought to be associated with deformation of the fore-arc enhanced by the subduction of fractured seamounts forming the Juan Fernandez ridge complex (THIERER *et al.* 2005). This is in agreement with the good correlation observed between the LCZs and the inception of HOFs (see Sect. 5.2) and suggests a link between the subducting plate structure, the mechanical behavior of the interface and the geodetic coupling coefficient. However, how HOFs may influence the mechanical behavior of the subduction fault remains unclear: the fracturation of the downgoing plate may directly favor fluid migration and modify the fluid pressure on the interface, but HOFs could also behave as barriers to sediment filling of the trench and modify the structure of the sedimentary prism directly involved in the faulting processes. In Chile, the latter effect is confirmed by the correlation observed between HOFs and positive gravity anomalies (e.g., SONG and SIMONS 2003; SOBIESIAK *et al.* 2007; ÁLVAREZ *et al.* 2014; MAKSYMOWICZ 2015). A relationship may exist between the interseismic coupling coefficient, the friction coefficient on the fault and the structure of the sedimentary prism as proposed for the Guerrero subduction zone by ROUSSET *et al.* (2015) or in the Maule area (CUBAS *et al.* 2013), but remains to be tested.

5.5. Creeping Low-Coupled Zones?

Since these swarms generally occur at the edges of LCZs, they could be an indirect sign that slow slip events (SSE) occur in the center of the LCZ and would reveal the existence of small-scale velocity-weakening patches located preferentially at the transition zone toward velocity-weakening dominant segments. This interpretation is consistent with observations made on several subduction zones where SSEs have been observed together with swarm seismicity (e.g., ROGERS and DRAGERT 2003; VALLEE *et al.* 2013); and with recent numerical models (e.g., HETLAND and SIMONS 2010; KANEKO *et al.* 2010).

However, no short-term SSE had been registered in these swarm-prone areas or elsewhere in Chile before the recent 2014 Iquique precursory sequence (RUIZ *et al.* 2014). This could be due to an observation bias since continuous GPS stations are operating in Chile only since 1995 for the oldest, and since 2004 for most of them, and that they are not homogeneously distributed over the Chilean coast. Indeed, most of the swarm sequences reported by HOLTKAMP *et al.* (2011) occurred before 1990, and only one cGPS station located far from the trench was operative during the 2006 Baranquilla swarm (Copiapó station, 27°S) showing no clear evidence for transient motion (COMTE *et al.* 2002; HOLTKAMP *et al.* 2011). The swarms that occurred since 2008 offshore Iquique (Fig. 4) were located in the less resolved part of the subduction zone, i.e., where the distance between the coast, the cGPS stations and the trench is the highest, preventing clear detection of associated SSE.

Nevertheless, since the widest well-resolved La Serena and Iquique LCZs are instrumented by dense cGPS networks since ~2004, we infer that no small-duration transient slip comparable to the Mexican or Cascadian SSEs that usually produce centimeters of displacements on c-GPS time-series has occurred there since 10 years (e.g., VERGNOLLE *et al.* 2010). If an Mw 6.5 SSE would occur in the very shallow part of the slab in the best-resolved part of our model, i.e., in front of the Tongoy Peninsula (30°S), it would produce a ~0.5 cm offset on the East component of the closest continuous GPS station and less than a millimeter displacement on North and Vertical

components (see supplementary figure 9). If spread over several months, such an event would probably remain hidden under the seasonal variations and remain undetected in the continuous time-series. Therefore, if creeping occurred in the La Serena LCZ, it must have been either very slow slip events (VSSE, RUIZ *et al.* 2014) occurring on tens of years, or short-term SSE that would remain beyond the detectability threshold of our network, i.e., on the shallowest part of the slab.

If all the swarm events detected in Chile by HOLTKAMP *et al.* (2011) are located at the segment-LCZ transition zones, not all LCZs have experienced swarms (Mejillones, Constitución, see Fig. 3). This lack of swarm activity during the interseismic period could be interpreted as an evidence for a smooth fault interface that could be creeping silently (HOLTKAMP and BRUDZINSKI 2014), while the number and intensity of swarms in the other LCZs may reflect the density of small-scale velocity-weakening asperities. It is also possible that in some cases, the activity of LCZs is controlled by the roughness of the subducted oceanic plate while in others, coupling is decreased by the connection between crustal fault networks and the subduction interface and not by a change in interface roughness. This could be the case for the Mejillones Peninsula LCZ where large crustal fault networks have been imaged and could reach the subduction interface inducing a lower coupling coefficient without swarm activity. However, we have probably missed some swarm sequences in the CSN catalog or the catalog is too short to get a representative swarm distribution, and therefore we cannot rule out the fact that swarms will occur in the vicinity of the Mejillones LCZ.

6. Conclusions

We derived an almost continuous distribution of interseismic coupling along the Chilean coast (18°–38°S) that reproduces reasonably well the GPS measurements conducted along the margin since the early 1990s. These data are overall consistent with highly variable coupling on the subduction zone and a clockwise rotation motion of the Andean sliver that produces 1 cm/year eastward motion in the Bolivian

Andes and few mm/year at the Maule region latitudes ($\sim 38^\circ\text{S}$).

The comparison between the interseismic coupling and the three large megathrust ruptures that struck Chile in the last 5 years confirms a very good correlation between high coseismic slip and high coupling, while ruptures stopped in LCZ. Therefore, coupling coefficient could be used as a good proxy to assess the location and shape of future megathrust ruptures, even if we still lack understanding on the timing of these ruptures and on their overall magnitude.

Detailed analysis of the background seismicity registered by the Chilean catalog (CSN) demonstrates that often, no simple relationship exists between the moderate seismicity and the coupling coefficient. The three Chilean seismic gaps exhibit very low rates of background seismicity that concentrate in intermediate-to-low coupling areas suggesting that highly coupled zones correspond to fully locked velocity-weakening asperities, but this relationship vanished in the Metropolitan or the Camarones segments.

Seismic swarms occur in general at the transition between highly coupled segments and low-coupled zones (LCZs), suggesting that LCZs behave as velocity-strengthening material sliding aseismically and triggering swarms on their vicinity. Even if no short-term SSE have been detected there in the last decade in Chile, LCZs and notably the La Serena area are probably experiencing either shallow undetected SSE or very long-term SSE ranging on several decades. Since most of these LCZs behaved as barriers to the propagation of past and recent megathrust earthquakes and could be involved in their nucleation process as it has been the case for the 2014 Mw 8.2 Iquique earthquake, they should be the focus of special attention by the community in the future.

Acknowledgments

We are grateful to all people that have been involved throughout the years in the field work and maintenance of the GPS network, in particular D. Carrizo, A. Delorme, S. Peyrat, C. Bermejo and I. Ortega. This work has been supported by LiA “Montessus de Ballore” and received partial support from Grants

ANR-2011-BS56-017 and ANR-2012-BS06-004 of the French "Agence Nationale de la Recherche (ANR)". GPS receivers for campaign measurements were provided by RESIF (Réseau sismologique français). We thank Rob McCaffrey for freely providing Tdefnode, and the Centro Sismologico Nacional of Universidad de Chile, Santiago, for making their catalog available. All the figures have been done using Generic Mapping Tools. We thank two anonymous reviewers for their useful comments on this work.

REFERENCES

- ÁLVAREZ, O., NACIF, S., GIMENEZ, M., FOLGUERA, A., and BRAITENBERG, C. (2014). *Goce derived vertical gravity gradient delineates great earthquake rupture zones along the chilean margin*. Tectonophysics, doi:[10.1016/j.tecto.2014.03.011](https://doi.org/10.1016/j.tecto.2014.03.011), 622:198–215.
- ARÁNGUIZ, R., GONZÁLEZ, G., GONZÁLEZ, J., CATALÁN, P.A., CIENFUEGOS, R., YAGI, Y., OKUWAKI, R., URRÁ, L., CONTRERAS, K., DEL RIO, I. *et al.* (2016) *The 16 September 2015 Chile Tsunami from the Post-Tsunami Survey and Numerical Modeling Perspectives*. Pure and Applied Geophysics, 1–16.
- ARGUS, D. F., GORDON, R. G., and DEMETS, C. (2011). *Geologically current motion of 56 plates relative to the no-net-rotation reference frame*. Geochemistry, Geophysics, Geosystems, doi:[10.1029/2011GC003751](https://doi.org/10.1029/2011GC003751), 12(11).
- ARMÍJO, R., RAULD, R., THIELE, R., VARGAS, G., CAMPOS, J., LACASSIN, R., and KAUSEL, E. (2010). *The west andean thrust, the san ramón fault, and the seismic hazard for santiago, chile*. Tectonics, doi:[10.1029/2008TC002427](https://doi.org/10.1029/2008TC002427), 29(2).
- ARMÍJO, R. and THIELE, R. (1990). *Active faulting in northern Chile: ramp stacking and lateral decoupling along a subduction plate boundary?* Earth and Planetary Science Letters, doi:[10.1016/0012-821X\(90\)90087-E](https://doi.org/10.1016/0012-821X(90)90087-E), 98(1):40–61.
- ARRIAGADA, C., ROPERCH, P., MPODOZIS, C., and COBBOLD, P. (2008). *Paleogene building of the bolivian orocline: Tectonic restoration of the central andes in 2-d map view*. Tectonics, doi:[10.1029/2008TC002269](https://doi.org/10.1029/2008TC002269), 27(6).
- BÉJAR-PIZARRO, M., CARRIZO, D., SOCQUET, A., ARMÍJO, R., BARRIENTOS, S., BONDoux, F., BONVALOT, S., CAMPOS, J., COMTE, D., DE CHABALIER, J., *et al.* (2009). *Asperities and barriers on the seismogenic zone in North Chile: state-of-the-art after the 2007 Mw 7.7 Tocopilla earthquake inferred by GPS and InSAR data*. Geophysical Journal International, doi:[10.1111/j.1365-246X.2010.04748.x](https://doi.org/10.1111/j.1365-246X.2010.04748.x).
- BÉJAR-PIZARRO, M., SOCQUET, A., ARMÍJO, R., CARRIZO, D., GENRICH, J., and SIMONS, M. (2013). *Andean structural control on interseismic coupling in the north chile subduction zone*. Nature Geoscience, doi:[10.1038/ngeo1802](https://doi.org/10.1038/ngeo1802), 6(6):462–467.
- BEVIS, M., KENDRICK, E., SMALLEY JR, R., BROOKS, B., ALLMENDINGER, R., and ISACKS, B. (2001). *On the strength of interplate coupling and the rate of back arc convergence in the central Andes: An analysis of the interseismic velocity field*. Geochemistry Geophysics Geosystems, doi:[10.1029/2001GC000198](https://doi.org/10.1029/2001GC000198), 2(11):1067.
- BEVIS, M., KENDRICK, E., SMALLEY JR, R., HERRING, T., GODOY, J., and GALBAN, F. (1999). *Crustal motion north and south of the Arica deflection: comparing recent geodetic results from the Central Andes*. Geochemistry Geophysics Geosystems, doi:[10.1029/1999GC000011](https://doi.org/10.1029/1999GC000011), 1(12):1005.
- BIE, L. and RYDER, I. (2015). *The 2005 tarapaca earthquake: a likely indirect trigger of the 2014 iquique earthquake*. In EGU General Assembly Conference Abstracts, volume 17, page 10013.
- BROOKS, B., BEVIS, M., SMALLEY JR, R., KENDRICK, E., MANCEDA, R., LAURÍA, E., MATURANA, R., and ARAUJO, M. (2003). *Crustal motion in the Southern Andes (26–36 S): Do the Andes behave like a microplate?* Geochemistry Geophysics Geosystems, doi:[10.1029/2003GC000505](https://doi.org/10.1029/2003GC000505), 4(10):1085.
- BROOKS, B., BEVIS, M., WHIPPLE, K., ARROWSMITH, J., FOSTER, J., ZAPATA, T., KENDRICK, E., MINAYA, E., ECHALAR, A., BLANCO, M., *et al.* (2011). *Orogenic-wedge deformation and potential for great earthquakes in the central andean backarc*. Nature Geoscience, doi:[10.1038/ngeo1143](https://doi.org/10.1038/ngeo1143), 4(6):380–383.
- BÜRGMANN, R., KOGAN, M. G., STEBLOV, G. M., HILLEY, G., LEVIN, V. E., and APEL, E. (2005). *Interseismic coupling and asperity distribution along the kamchatka subduction zone*. Journal of Geophysical Research: Solid Earth, doi:[10.1029/2005JB003648](https://doi.org/10.1029/2005JB003648), 110(B7).
- CALISTO, I., MILLER, M., and CONSTANZO, I. (2016). *Comparison between tsunami signals generated by different source models and the observed data of the illapel 2015 earthquake*. Pure and Applied Geophysics, pages 1–11.
- CHLIEH, M., AVOUAC, J., SIEH, K., NATAWIDJAJA, D. H., and GALETZKA, J. (2008). *Heterogeneous coupling of the sumatran megathrust constrained by geodetic and paleogeodetic measurements*. Journal of Geophysical Research: Solid Earth (1978–2012), doi:[10.1029/2007JB004981](https://doi.org/10.1029/2007JB004981), 113(B5).
- CHLIEH, M., PERFETTINI, H., TAVERA, H., AVOUAC, J., REMY, D., NOCQUET, J., ROLANDONE, F., BONDoux, F., GABALDA, G., and BONVALOT, S. (2011). *Interseismic coupling and seismic potential along the central andes subduction zone*. Journal of Geophysical Research, doi:[10.1029/2010JB008166](https://doi.org/10.1029/2010JB008166), 116(B12):B12405.
- COMTE, D., HAESSLER, H., DORBATH, L., PARDO, M., MONFRET, T., LAVENU, A., PONTOISE, B., and HELLO, Y. (2002). *Seismicity and stress distribution in the copiapó, northern chile subduction zone using combined on-and off-shore seismic observations*. Physics of the earth and planetary interiors, doi:[10.1016/S0031-9201\(02\)00052-3](https://doi.org/10.1016/S0031-9201(02)00052-3), 132(1):197–217.
- COMTE, D. and PARDO, M. (1991). *Reappraisal of great historical earthquakes in the northern Chile and southern Peru seismic gaps*. Natural Hazards, 4(1):23–44.
- CONTRERAS-REYES, E. and CARRIZO, D. (2011). *Control of high oceanic features and subduction channel on earthquake ruptures along the chile–peru subduction zone*. Physics of the Earth and Planetary Interiors, doi:[10.1016/j.pepi.2011.03.002](https://doi.org/10.1016/j.pepi.2011.03.002), 186(1):49–58.
- CUBAS, N., AVOUAC, J., SOULOUMIAC, P., and LEROY, Y. (2013). *Megathrust friction determined from mechanical analysis of the forearc in the maule earthquake area*. Earth and Planetary Science Letters, doi:[10.1016/j.epsl.2013.07.037](https://doi.org/10.1016/j.epsl.2013.07.037), 381:92–103.
- DEMETS, C., GORDON, R. G., ARGUS, D. F., and STEIN, S. (1994). *Effect of recent revisions to the geomagnetic reversal time scale*

- on estimates of current plate motions. Geophysical research letters, doi:[10.1029/94GL02118](https://doi.org/10.1029/94GL02118), 21(20):2191–2194.
- DUCRET, G., DOIN, M., GRANDIN, R., SOCQUET, A., VIGNY, C., MÉTOIS, M., and BÉJAR-PIZZARO, M. (2012). Measurement of interseismic strain accumulation in the southern andes (25°–35°s) using envisat sar data. In EGU General Assembly Conference Abstracts, volume 14, page 10391.
- DURAND, V., BOUCHON, M., FLOYD, M. A., THEODULIDIS, N., MARSAN, D., KARABULUT, H., and SCHMITTBUHL, J. (2014). *Observation of the spread of slow deformation in greece following the breakup of the slab*. Geophysical Research Letters, doi:[10.1002/2014GL061408](https://doi.org/10.1002/2014GL061408), 41(20):7129–7134.
- GARDNER, J. and KNOPOFF, L. (1974). *Is the sequence of earthquakes in southern california, with aftershocks removed, poissonian*. Bull. Seismol. Soc. Am., 64(5):1363–1367.
- HAYES, G. P., WALD, D. J., and JOHNSON, R. L. (2012). *Slab1. 0: A three-dimensional model of global subduction zone geometries*. Journal of Geophysical Research: Solid Earth (1978–2012), doi:[10.1029/2011JB008524](https://doi.org/10.1029/2011JB008524), 117(B1).
- HETLAND, E. and SIMONS, M. (2010). *Post-seismic and interseismic fault creep II: transient creep and interseismic stress shadows on megathrusts*. Geophysical Journal International, doi:[10.1111/j.1365-246X.2009.04482.x](https://doi.org/10.1111/j.1365-246X.2009.04482.x), 181(1):99–112.
- HOFFMANN-ROTHER, A., KUKOWSKI, N., DRESEN, G., ECHTLER, H., ONCKEN, O., KLOTZ, J., SCHEUBER, E., and KELLNER, A. (2006). *Oblique convergence along the Chilean margin: partitioning, margin-parallel faulting and force interaction at the plate interface*. The Andes, pages 125–146.
- HOLTKAMP, S. and BRUDZINSKI, M. R. (2014). *Megathrust earthquake swarms indicate frictional changes which delimit large earthquake ruptures*. Earth and Planetary Science Letters, doi:[10.1016/j.epsl.2013.10.033](https://doi.org/10.1016/j.epsl.2013.10.033), 390:234–243.
- HOLTKAMP, S. G., PRITCHARD, M., and LOHMAN, R. (2011). *Earthquake swarms in South America*. Geophysical Journal International, doi:[10.1111/j.1365-246X.2011.05137.x](https://doi.org/10.1111/j.1365-246X.2011.05137.x), 187(1):128–146.
- KANEKO, Y., AVOUAC, J., and LAPUSTA, N. (2010). *Towards inferring earthquake patterns from geodetic observations of interseismic coupling*. Nature Geoscience, doi:[10.1038/ngeo843](https://doi.org/10.1038/ngeo843), 3(5):363–369.
- KATO, A. and NAKAGAWA, S. (2014). *Multiple slow-slip events during a foreshock sequence of the 2014 iquique, chile Mw 8.1 earthquake*. Geophysical Research Letters, doi:[10.1002/2014GL061138](https://doi.org/10.1002/2014GL061138), 41(15):5420–5427.
- KATO, A., OBARA, K., IGARASHI, T., TSURUOKA, H., NAKAGAWA, S., and HIRATA, N. (2012). *Propagation of slow slip leading up to the 2011 mw 9.0 tohoku-oki earthquake*. Science, doi:[10.1126/science.1215141](https://doi.org/10.1126/science.1215141), 335(6069):705–708.
- KAUSEL, E. and CAMPOS, J. (1992). *The Ms= 8 tensional earthquake of 9 december 1950 of northern chile and its relation to the seismic potential of the region*. Physics of the earth and planetary interiors, doi:[10.1016/0031-9201\(92\)90203-8](https://doi.org/10.1016/0031-9201(92)90203-8), 72(3):220–235.
- KENDRICK, E., BEVIS, M., SMALLEY, R., and BROOKS, B. (2001). *An integrated crustal velocity field for the central Andes*. Geochem. Geophys. Geosyst, doi:[10.1029/2001GC000191](https://doi.org/10.1029/2001GC000191), 2(11):1066.
- KHAZARADZE, G. and KLOTZ, J. (2003). *Short-and long-term effects of GPS measured crustal deformation rates along the south central Andes*. Journal of geophysical research, doi:[10.1029/2002JB008179](https://doi.org/10.1029/2002JB008179), 108(B6):2289.
- KLEIN, E., FLEITOUT, L., VIGNY, C., and GARAU, J. (2016). *Afterslip and viscoelastic relaxation model inferred from the large scale postseismic deformation following the 2010 Mw 8,8 Maule earthquake (Chile)*. Accepted for publication in Geophysical Journal International.
- KLOTZ, J., KHAZARADZE, G., ANGERMANN, D., REIGBER, C., PERDOMO, R., and CIFUENTES, O. (2001). *Earthquake cycle dominates contemporary crustal deformation in Central and Southern Andes*. Earth and Planetary Science Letters, doi:[10.1016/S0012-821X\(01\)00532-5](https://doi.org/10.1016/S0012-821X(01)00532-5), 193(3–4):437–446.
- KONCA, A., AVOUAC, J., SLADEN, A., MELTZNER, A., SIEH, K., FANG, P., LI, Z., GALETZKA, J., GENRICH, J., CHLIEH, M., et al. (2008). *Partial rupture of a locked patch of the Sumatra megathrust during the 2007 earthquake sequence*. Nature, doi:[10.1038/nature07572](https://doi.org/10.1038/nature07572), 456(7222):631–635.
- LAY, T., YUE, H., BRODSKY, E. E., and AN, C. (2014). *The 1 April 2014 Iquique, Chile, Mw 8.1 earthquake rupture sequence*. Geophysical Research Letters, doi:[10.1002/2014GL060238](https://doi.org/10.1002/2014GL060238), 41(11):3818–3825.
- LI, S., MORENO, M., BEDFORD, J., ROSENAU, M., and ONCKEN, O. (2015). *Revisiting visco-elastic effects on interseismic deformation and locking degree: a case study of the Peru-North Chile subduction zone*. Journal of Geophysical Research: Solid Earth, doi:[10.1002/2015JB011903](https://doi.org/10.1002/2015JB011903).
- LOMNITZ, C. (1970). *Major earthquakes and tsunamis in Chile during the period 1535 to 1955*. International Journal of Earth Sciences, 59(3):938–960.
- LOVELESS, J. and MEADE, B. (2011). *Spatial correlation of interseismic coupling and coseismic rupture extent of the 2011 Mw9.0 Tohoku-Oki earthquake*. Geophys. Res. Lett, doi:[10.1029/2011GL048561](https://doi.org/10.1029/2011GL048561), 38:L17306.
- MAKSYMOWICZ, A. (2015). *The geometry of the Chilean continental wedge: Tectonic segmentation of subduction processes off Chile*. Tectonophysics, doi:[10.1016/j.tecto.2015.08.007](https://doi.org/10.1016/j.tecto.2015.08.007), 659:183–196.
- MAROT, M., MONFRET, T., GERBAULT, M., NOLET, G., RANALLI, G., and PARDO, M. (2014). *Flat versus normal subduction zones: a comparison based on 3-d regional travelttime tomography and petrological modelling of central chile and western Argentina (29°–35°s)*. Geophysical Journal International, doi:[10.1093/gji/ggu355](https://doi.org/10.1093/gji/ggu355), 199(3):1633–1654.
- MCCAFFREY, R. (2002). *Crustal block rotations and plate coupling*. Plate Boundary Zones, Geodyn. Ser, doi:[10.1029/GD030p0101](https://doi.org/10.1029/GD030p0101), 30:101–122.
- MCCAFFREY, R. (2009). *Time-dependent inversion of three-component continuous gps for steady and transient sources in northern Cascadia*. Geophysical Research Letters, doi:[10.1029/2008GL036784](https://doi.org/10.1029/2008GL036784), 36(7).
- MCCAFFREY, R. (2014). *Interseismic locking on the Hikurangi subduction zone: Uncertainties from slow-slip events*. Journal of Geophysical Research: Solid Earth, doi:[10.1002/2014JB010945](https://doi.org/10.1002/2014JB010945), 119(10):7874–7888.
- MELNICK, D. and BOOKHAGEN, B. (2009). *Segmentation of megathrust rupture zones from fore-arc deformation patterns over hundreds to millions of years, Arauco peninsula, Chile*. Journal of Geophysical Research. B. Solid Earth, doi:[10.1029/2008JB005788](https://doi.org/10.1029/2008JB005788), 114.
- MÉTOIS, M., SOCQUET, A., and VIGNY, C. (2012). *Interseismic coupling, segmentation and mechanical behavior of the central chile subduction zone*. Journal of Geophysical Research, doi:[10.1029/2011JB008736](https://doi.org/10.1029/2011JB008736), 117(B3).
- MÉTOIS, M., SOCQUET, A., VIGNY, C., CARRIZO, D., PEYRAT, S., DELORME, A., MAUREIRA, E., VALDERAS-BERMEJO, M.-C., and ORTEGA, I. (2013). *Revisiting the north chile seismic gap*

- segmentation using gps-derived interseismic coupling. *Geophysical Journal International*, doi:[10.1093/gji/ggt183](https://doi.org/10.1093/gji/ggt183), 194(3):1283–1294.
- MÉTOIS, M., VIGNY, C., SOCQUET, A., DELORME, A., MORVAN, S., ORTEGA, I., and VALDERAS-BERMEJO, C.-M. (2014). *GPS-derived interseismic coupling on the subduction and seismic hazards in the Atacama region, Chile*. *Geophysical Journal International*, doi:[10.1093/gji/ggt418](https://doi.org/10.1093/gji/ggt418), 196(2):644–655.
- MORENO, M., KLOTZ, J., MELNICK, D., ECHTLER, H., and BATAILLE, K. (2008). *Active faulting and heterogeneous deformation across a megathrust segment boundary from GPS data, south central Chile (36–39 S)*. *Geochem. Geophys. Geosyst.*, doi:[10.1029/2008GC002198](https://doi.org/10.1029/2008GC002198), 9:36–39.
- MORENO, M., ROSENAU, M., and ONKEN, . (2010). *2010 Maule earthquake slip correlates with pre-seismic locking of Andean subduction zone*. *Nature*, doi:[10.1038/nature09349](https://doi.org/10.1038/nature09349), 467.
- MULLER, R., ROEST, W., ROYER, J., GAHAGAN, L., and SCLATER, J. (1997). *Digital isochrons of the world's ocean floor*. *Journal of Geophysical Research*, doi:[10.1029/96JB01781](https://doi.org/10.1029/96JB01781), 102(B2):3211–3214.
- NOCQUET, J., VILLEGAS-LANZA, J., CHLIEH, M., MOTHES, P., ROLANDONE, F., JARRIN, P., CISNEROS, D., ALVARADO, A., AUDIN, L., BONDOUX, F., et al. (2014). *Motion of continental slivers and creeping subduction in the northern Andes*. *Nature Geoscience*, doi:[10.1038/NNGEO2099](https://doi.org/10.1038/NNGEO2099), 7(4):287–291.
- NORABUENA, E., LEFFLER-GRIFFIN, L., MAO, A., DIXON, T., STEIN, S., SACKS, I., OCOLA, L., and ELLIS, M. (1998). *Space geodetic observations of Nazca-South America convergence across the central Andes*. *Science*, doi:[10.1126/science.279.5349.358](https://doi.org/10.1126/science.279.5349.358), 279(5349):358.
- OKADA, Y. (1985). *Surface deformation due to shear and tensile faults in a half-space*. *Bulletin of the Seismological Society of America*, 75(4):1135–1154.
- REILINGER, R. and KADINSKY-CADE, K. (1985). *Earthquake deformation cycle in the Andean back arc, western Argentina*. *Journal of Geophysical Research*, doi:[10.1029/JB090iB14p12701](https://doi.org/10.1029/JB090iB14p12701), 90(B14):12701–12.
- ROGERS, G. and DRAGERT, H. (2003). *Episodic tremor and slip on the Cascadia subduction zone: The chatter of silent slip*. *Science*, doi:[10.1126/science.1084783](https://doi.org/10.1126/science.1084783), 300(5627):1942–1943.
- ROUSSET, B., LASSERRE, C., CUBAS, N., GRAHAM, S., RADIGUET, M., DEMETS, C., SOCQUET, A., CAMPILLO, M., KOSTOGLODOV, V., CABRAL-CANO, E., et al. (2015). *Lateral variations of interplate coupling along the mexican subduction interface: Relationships with long-term morphology and fault zone mechanical properties*. *Pure and Applied Geophysics*, pages 1–20.
- RUEGG, J., RUDLOFF, A., VIGNY, C., MADARIAGA, R., DE CHABALIER, J., CAMPOS, J., KAUSEL, E., BARRIENTOS, S., and DIMITROV, D. (2009). *Interseismic strain accumulation measured by GPS in the seismic gap between Constitución and Concepción in Chile*. *Physics of the Earth and planetary interiors*, doi:[10.1016/j.pepi.2008.02.015](https://doi.org/10.1016/j.pepi.2008.02.015), 175(1–2):78–85.
- RUIZ, S., KLEIN, E., DEL CAMPO, F., RIVERA, E., POLI, P., MÉTOIS, M., VIGNY, C., BAEZ, J., VARGAS, J., LEYTON, F., MADARIAGA, R., and FLEITOUT, L. (2016). *The Illapel Mw 8.3 earthquake triggered by deep transient slow slip*. Accepted in *Seismological research letters*.
- RUIZ, S., MÉTOIS, M., FUENZALIDA, A., RUIZ, J., LEYTON, F., GRANDIN, R., VIGNY, C., MADARIAGA, R., and CAMPOS, J. (2014). *Intense foreshocks and a slow slip event preceded the 2014 Iquique Mw 8.1 earthquake*. *Science*, doi:[10.1126/science.1256074](https://doi.org/10.1126/science.1256074), 345(6201):1165–1169.
- SATO, M., ISHIKAWA, T., UJIHARA, N., YOSHIDA, S., FUJITA, M., MOCHIZUKI, M., and ASADA, A. (2011). *Displacement above the hypocenter of the 2011 tohoku-oki earthquake*. *Science*, doi:[10.1126/science.1207401](https://doi.org/10.1126/science.1207401), 332(6036):1395–1395.
- SAVAGE, J. (1983). *A dislocation model of strain accumulation and release at a subduction zone*. *Journal of Geophysical Research-Solid Earth*, doi:[10.1029/JB088iB06p04984](https://doi.org/10.1029/JB088iB06p04984), 88(B6).
- SCHURR, B., ASCH, G., HAINZL, S., BEDFORD, J., HOECHNER, A., PALO, M., WANG, R., MORENO, M., BARTSCH, M., ZHANG, Y., et al. (2014). *Gradual unlocking of plate boundary controlled initiation of the 2014 Iquique earthquake*. *Nature*.
- SIMONS, M., MINSON, S. E., SLADEN, A., ORTEGA, F., JIANG, J., OWEN, S. E., MENG, L., AMPUERO, J., WEI, S., CHU, R., et al. (2011). *The 2011 Magnitude 9.0 Tohoku-Oki earthquake: Mosaicking the megathrust from seconds to centuries*. *Science*, doi:[10.1126/science.1206731](https://doi.org/10.1126/science.1206731), 332(6036):1421–1425.
- SOBIESIAK, M., MEYER, U., SCHMIDT, S., GÖTZE, H.-J., and KRAWCZYK, C. (2007). *Asperity generating upper crustal sources revealed by b value and isostatic residual anomaly grids in the area of antofagasta, Chile*. *Journal of Geophysical Research: Solid Earth*, doi:[10.1029/2006JB004796](https://doi.org/10.1029/2006JB004796), 112(B12).
- SONG, T. and SIMONS, M. (2003). *Large trench-parallel gravity variations predict seismogenic behavior in subduction zones*. *Science*, doi:[10.1126/science.1085557](https://doi.org/10.1126/science.1085557), 301(5633):630–633.
- TASSARA, A., GOTZE, H., SCHMIDT, S., and HACKNEY, R. (2006). *Three-dimensional density model of the Nazca plate and the Andean continental margin*. *Journal of Geophysical Research-Solid Earth*, doi:[10.1029/2005JB003976](https://doi.org/10.1029/2005JB003976), 111(B9).
- THIERER, P., FLUEH, E., KOPP, H., TILMANN, F., COMTE, D., and CONTRERAS, S. (2005). *Local earthquake monitoring offshore Valparaíso, Chile*. *N. Jb. Geol. Paläont. Abh.*, 236(1/2):173–183.
- TRUBIENKO, O., FLEITOUT, L., GARAUD, J., and VIGNY, C. (2013). *Interpretation of interseismic deformations and the seismic cycle associated with large subduction earthquakes*. *Tectonophysics*, doi:[10.1016/j.tecto.2012.12.027](https://doi.org/10.1016/j.tecto.2012.12.027), 589:126–141.
- VALLEE, M., NOCQUET, J., BATTAGLIA, J., FONT, Y., SEGOVIA, M., REGNIER, M., MOTHES, P., JARRIN, P., CISNEROS, D., VACA, S., et al. (2013). *Intense interface seismicity triggered by a shallow slow slip event in the central Ecuador subduction zone*. *Journal of Geophysical Research: Solid Earth*, doi:[10.1002/jgrb.50216](https://doi.org/10.1002/jgrb.50216), 118(6):2965–2981.
- VARGAS, G., KLINGER, Y., ROCKWELL, T., FORMAN, S., REBOLLEDO, S., BAIZE, S., LACASSIN, R., and ARMJO, R. (2014). *Probing large intraplate earthquakes at the west flank of the Andes*. *Geology*, doi:[10.1130/G35741.1](https://doi.org/10.1130/G35741.1), 42(12):1083–1086.
- VERGNOLLE, M., WALPERSDORF, A., KOSTOGLODOV, V., TREGONING, P., SANTIAGO, J., COTTE, N., and FRANCO, S. (2010). *Slow slip events in Mexico revised from the processing of 11 year gps observations*. *Journal of Geophysical Research: Solid Earth* (1978–2012), doi:[10.1029/2009JB006852](https://doi.org/10.1029/2009JB006852), 115(B8).
- VIGNY, C., RUDLOFF, A., RUEGG, J., MADARIAGA, R., CAMPOS, J., and ALVAREZ, M. (2009). *Upper plate deformation measured by GPS in the Coquimbo Gap, Chile*. *Physics of the Earth and Planetary Interiors*, doi:[10.1016/j.pepi.2008.02.013](https://doi.org/10.1016/j.pepi.2008.02.013), 175(1–2):86–95.
- VIGNY, C., SOCQUET, A., PEYRAT, S., RUEGG, J.-C., MÉTOIS, M., MADARIAGA, R., MORVAN, S., LANCIERI, M., LACASSIN, R., CAMPOS, J., CARRIZO, D., BEJAR-PIZARRO, M., BARRIENTOS, S., ARMJO, R., ARANDA, C., VALDERAS-BERMEJO, M.-C., ORTEGA, I., BONDOUX, F., BAIZE, S., LYON-CAEN, H., PAVEZ, A., VILOTTE, J. P., BEVIS, M.,

- BROOKS, B., SMALLEY, R., PARRA, H., BAEZ, J.-C., BLANCO, M., CIMBARO, S., and KENDRICK, E. (2011). *The 2010 Mw 8.8 Maule megathrust earthquake of Central Chile, monitored by GPS*. Science, doi:[10.1126/science.1204132](https://doi.org/10.1126/science.1204132), 332(6036):1417–21.
- WALLACE, L., BEAVAN, J., McCAFFREY, R., and DARBY, D. (2004). *Subduction zone coupling and tectonic block rotations in the North Island, New Zealand*. Journal of Geophysical Research, doi:[10.1029/2004JB003241](https://doi.org/10.1029/2004JB003241), 109(B12):B12406.
- WANG, K. and BILEK, S. L. (2014). *Invited review paper: Fault creep caused by subduction of rough seafloor relief*. Tectonophysics, doi:[10.1016/j.tecto.2013.11.024](https://doi.org/10.1016/j.tecto.2013.11.024), 610:1–24.
- YE, L., LAY, T., KANAMORI, H., and KOPER, K. (2015). *Rapidly estimated seismic source parameters for the 16 september 2015 Illapel, Chile Mw 8.3 earthquake*. Pure and Applied Geophysics, pages 1–12.
- YOSHIOKA, S., WANG, K., and MAZZOTTI, S. (2005). *Interseismic locking of the plate interface in the Northern Cascadia subduction zone, inferred from inversion of GPS data*. Earth and Planetary Science Letters, doi:[10.1016/j.epsl.2004.12.018](https://doi.org/10.1016/j.epsl.2004.12.018), 231(3):239–247.

(Received December 8, 2015, revised March 16, 2016, accepted March 19, 2016, Published online April 4, 2016)